Dedicated Global Optimization Search for Ground State Silica Nanoclusters: $(SiO_2)_N$ ($N = 6-12$)

E. Flikkema and S. T. Bromley*

Ceramic Membrane Centre "The Pore", Delft University of Technology, Julianalaan 136, 2628 BL Delft, The Netherlands

Received: January 15, 2004; In Final Form: April 14, 2004

Employing a polyatomic version of the basin hopping global optimization algorithm, together with interatomic potentials specifically tailored to accurately describe the structures and energetics of nanoscale silica, a large number of energetically low-lying nanoclusters for $(SiO_2)_N$ ($N = 6-12$) was generated. Substantial subsets of particularly low-energy candidate structures for each cluster size were subsequently further evaluated using density functional theory (DFT) energy minimization calculations. We report the resulting lowest energy nanoclusters, together with the energetically nearest lying nanoclusters, for each cluster class, $(SiO_2)_N$ ($N = 6-12$). The majority of the clusters obtained display no structural motifs typical of bulk crystalline silica. Of all the clusters studied, the lowest energy $(SiO_2)_8$ cluster found is shown to be especially thermodynamically favored compared to other similarly sized cluster isomers and with respect to addition or removal of SiO_2 units. The clusters are discussed with respect to their structure, their reactivity, and their suitability as building blocks for new materials.

Introduction

Bulk silica (SiO_2) displays a great wealth of natural and synthetic polymorphic forms with the relative thermodynamic stability of each relatively well established. In stark contrast, although silica is increasingly being fabricated into discrete nanoscale structures (e.g. nanotubes[1,2] and nanospheres[3,4]) and bulk silica modified with nanoscale precision (e.g. thin films,[5] nanopores,[6] and mesoporous silicas[7]), the low-energy landscape of nanoscale silica is relatively unknown. From a technological viewpoint both bottom-up and top-down approaches to silica nanomodification are providing a range of new potential applications (e.g. subwavelength photonics,[8,9] drug delivery systems,[10] and ultralow-*k* gate oxides[11]). A number of studies in the literature have explored the properties of isomers of small stoichiometric silica clusters using various combinations of structure derivation and energy minimization: (i) extensive manual searches with results energy-minimized using density functional theory (DFT),[12−14] or bulk-parametrized interatomic potentials,[15] (ii) deliberate manual design using repeated subunits with structures energy-minimized using DFT,[16] (iii) annealing of bulk silica fragments using classical molecular dynamics with bulk-parametrized interatomic potentials, followed by DFT energy minimization.[17] From these, and similar studies, although many silica nanocluster energies and structures have been evaluated, it is widely recognized that the ground state structures of only the five smallest nanoclusters, that is, $(SiO_2)_N$ ($N = 2-6$), have been relatively well established, all having a similar linear chain form. Cluster beam experiments obtaining $(SiO_2)_N$ $N = 2-4$ cluster anions with a chain form as the predominant low energy stoichiometric cluster type[18] have also tended to confirm this result. Recently, we proposed a new ground-state structure for $(SiO_2)_7$ that has a form quite different from the chain. To obtain this result we coupled our nanoscale silica interatomic potential with a genetic algorithm global optimization method to generate low-energy candidate structures, followed by DFT energy minimizations to accurately evaluate their energies.[19] In this extended investigation we apply our efficient methodology, with the alternative basin hopping (BH) global optimization strategy, to the exponentially increasingly complex phase space of $(SiO_2)_N$ nanoclusters, for $N = 6-12$, and propose new ground-state structures. All reported nanocluster $(SiO_2)_N$ structures are lower, or at most equal, in energy to all other correspondingly-sized structures previously reported in the literature.

Computational Methodology. Following our previous study, we employ our recently developed interatomic potential set,[19] which is specifically parametrized to accurately predict the energies and structures of silica nanoclusters. Since there are two atom types (Si and O) the interatomic potential consists of three potentials (Si−Si, O−O, and Si−O), each of Buckingham form, combined with electrostatic interactions. In this paper we combine our interatomic potentials with the Basin Hopping (BH) global optimization algorithm[20] to search for low-lying minima on the silica nanocluster energy landscape. The BH algorithm uses a combination of Metropolis Monte Carlo sampling and energy minimization to sample the phase space of cluster configurations. We base our implementation of the BH algorithm on the GMIN program by Wales and Doye.[21] As the original program is limited in its immediate application to monoelemental clusters, we have extended the program to be able to treat systems with multiple elements (i.e., Si and O). An additional hard-core potential was also introduced to all potentials to prevent atoms from falling on top of each other, during a BH run, due to the unphysical infinite attractive well, inherent to the Buckingham potential form, for very short distances. In a typical BH run two parameters need to be specified: the step size Δ (controlling the maximum change in structure per BH step) and the temperature *T*. These parameters need to be carefully tuned in order to achieve a maximum

* To whom correspondence should be addressed. E-mail: S.T.Bromley@tnw.tudelft.nl.

10.1021/jp049783r CCC: $27.50
Published on Web 06/19/2004

sampling efficiency. If the temperature T is too high the BH procedure is not sufficiently directed toward low-energy structures, whereas if the temperature is too low there is a risk of remaining trapped in a local minimum. If the step size Δ is too small the sampling procedure is inefficient, since many steps are needed to get an appreciable change in structure. If the step size is too large many of the changes will be rejected (according to a Metropolis[22] criterion). Another important issue is the choice of the initial coordinates. In principle it should not matter, since if the run is sufficiently long all of the phase space of cluster configurations is sampled. In reality the length of each run is limited, and the form of the energy landscape dictates the extent of the sampling achieved.[23] Although the BH algorithm is one of the least-hindered global optimization methods with respect to the specific topology of the potential energy surface,[24] to overcome such problems a selection of different starting structures can be made to help ensure an even and extensive phase space sampling.[20] For each of our BH runs, for $(SiO_2)_N$ ($N = 6-12$), the $(SiO_2)_N$ chain and a number of randomly generated cluster structures, of the respective size, were used as starting structures. It was found that for the smaller clusters $(SiO_2)_N$ ($N < 9$) only 2−3 random structures seemed to suffice to saturate the search; that is, using more random structures did not lead to further low-energy clusters, whereas for larger clusters up to eight random starting structures seemed to be sufficient to achieve saturation. For each cluster size production runs were performed using a fixed temperature (14,000 K) with the step size allowed to vary in each case in order to achieve an acceptance ratio of approximately 0.63. Both the temperature and acceptance ratio ranges were chosen according to a series of test runs for the mid-sized $(SiO_2)_9$ system for temperatures ranging from 9,000 K to 23,000 K and for acceptance ratios from 0.5 to 0.8. The parameters chosen were found to be optimal with respect to the energies of the clusters generated and number of low energy clusters generated. Further to these relatively high-temperature production runs, for $(SiO_2)_N$ ($N = 10-12$) we also found it useful to take selected low-energy cluster structures from completed BH runs as starting points for subsequent runs, using relatively lower temperatures (9,000 K), to specifically sample low-energy regions of phase space. The length of a typical production run was 10^6 steps and, for each run, the 200 lowest energy structures encountered were stored in a continuously updated file.

To accurately assess the energies of the clusters resulting from the BH procedure, taking into account the small root-mean-square (RMS) fluctuations in the relative energetic predictions of the FB potential with respect to the DFT energy evaluations (see below), a subset of 25−30 clusters, including the lowest energy 20 clusters and 5−10 higher energy high-symmetry clusters, were energy minimized using DFT. For all DFT calculations the B3LYP hybrid exchange-correlation functional,[25] together with a 6-31G(d) basis set, was used, employing no symmetry constraints. This level of theory has been shown in numerous previous studies to be suitable for calculating accurate structures and energies of silica nanoclusters.[12−14] All energies quoted are total energies, or energies with respect to that of the SiO_2 molecule, which allows us to directly compare energies from the interatomic-potential-based BH runs with the corresponding energies from our DFT energy minimizations. The GAMESS−UK[26] code was used for all DFT calculations.

Results

Suitability of the FB Potential. The FB potential gives a good account of the structures and relative energies of different silica nanoclusters and accurately reproduces the detailed binding energy trend of the lowest energy clusters (as energy minimized by DFT) for $(SiO_2)_N$ ($N = 2-12$); see Figure 1. The absolute values of the binding energies predicted by the FB potential are consistently somewhat higher, ∼15% with respect to the DFT results which, considering the neglect of electronic degrees of freedom, the simplicity of the potential form, and the diversity of silica structures considered, is gratifyingly good.

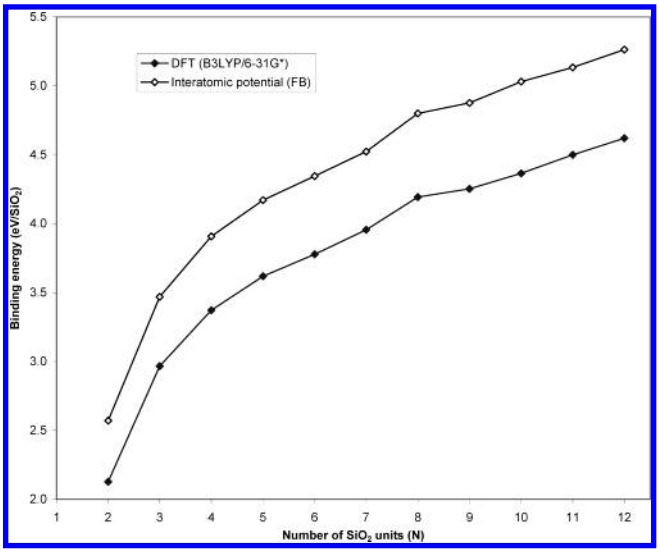

Figure 1. Comparison of the binding energies of the lowest energy clusters $(SiO_2)_N$ ($N = 2-12$) using clusters minimized using both DFT and the FB potential. Clusters 1−6 are two-ring chains and clusters 7−12 are those found by our combined BH/DFT methodology (see Figures 4-7). The binding energy is taken to be the difference between the total energy of the cluster $(SiO_2)_N$ and the energy of N isolated SiO_2 monomers, i.e., $BE = [E[(SiO_2)_N] - N.E(SiO_2)]/N$.

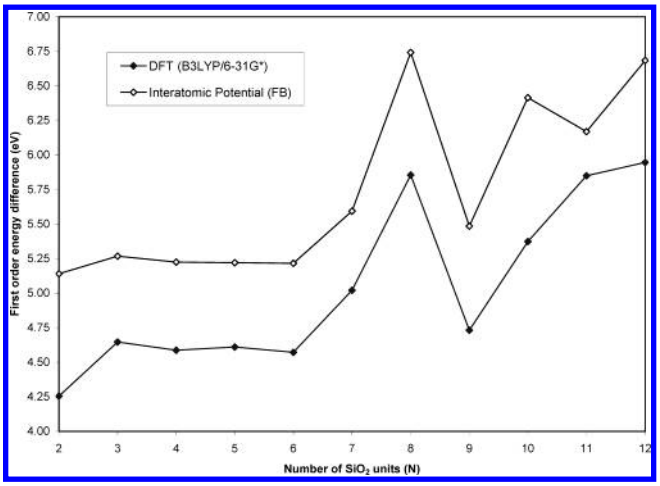

Figure 2. The first-order energy difference, ΔE, of the lowest energy clusters $(SiO_2)_N$ ($N = 2-12$) using clusters minimized using both DFT and the FB potential. We define ΔE as the difference between the total energy of cluster $(SiO_2)_N$ and that of the cluster $(SiO_2)_{N-1}$ together with that of one isolated SiO_2 monomer, i.e., $\Delta E = E[(SiO_2)_N] - E[(SiO_2)_{N-1}] - E(SiO_2)$.

Looking in more detail at the relative stabilities of the lowest-energy clusters, the first-order energy differences, that is, the energy difference between a cluster $(SiO_2)_{N+1}$ and the combined energies of the cluster $(SiO_2)_N$ and an isolated SiO_2 monomer, is also calculated using the FB potential and DFT. In Figure 2 it can be seen that the specific pattern of DFT-calculated energy differences is well reproduced by the FB potential (again a consistent difference between the two data sets of ∼15%) with only a small discrepancy for $(SiO_2)_{11}$. Finally, as a sensitive

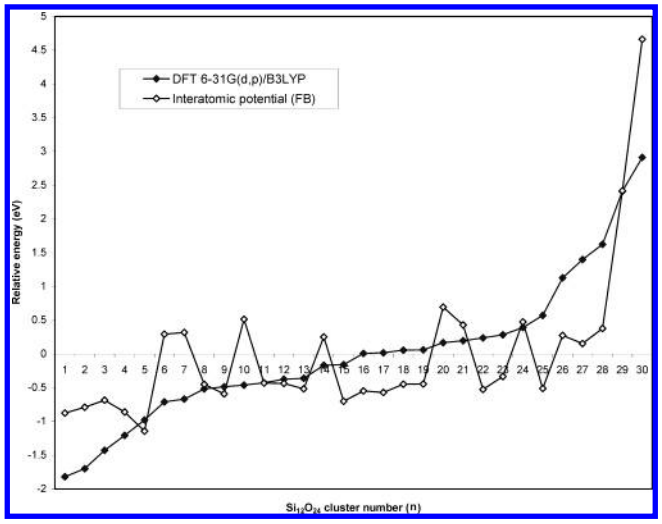

Figure 3. Total energies of the lowest 25 energy $(SiO_2)_{12}$ clusters as found by the BH procedure together with the energies of a further 5 symmetric clusters. The energies of these clusters as calculated by the FB interatomic potential are compared with the corresponding energies as calculated using DFT. We note that the lowest energy $(SiO_2)_{12}$ we could find in the literature is cluster $n = 10$,[17] which is found to have a DFT-minimized energy 1.36 eV above our lowest energy $(SiO_2)_{12}$ cluster.

test of the FB potential, we compare the relative energies predicted by the FB potential with those calculated by DFT energy minimization for a set of clusters within the same size class. In Figure 3 the relative energies of the 25 lowest energy $(SiO_2)_{12}$ clusters as found by our FB/BH methodology and a further 5 clusters having high symmetry, are shown along with the respective DFT-calculated relative energies. As we are only interested in the comparison of relative energies, in Figure 3 a vertical shift is applied to the curves to minimize the sum of squares between the two data sets. Calculating the resulting RMS deviation of the FB-predicted relative energies from those calculated by DFT energy-minimization yields a value of 0.06 eV/SiO_2. This value compares well with that previously calculated using a diverse set of $(SiO_2)_7$ clusters (0.07 eV/SiO_2[19]). Considering that the 25 lowest energy clusters, as calculated by DFT energy minimization, are typically found to span a range $\sim$0.15−0.25 eV/SiO_2, we can be reasonably assured that for each cluster size the ground-state cluster (if accessible by the BH global optimization method employed) is within this set.

We further note that in both our previous $(SiO_2)_7$ study[19] and in the present FB potential assessment, using considerably larger and more complex $(SiO_2)_{12}$ clusters, the lowest energy DFT-calculated cluster is found to correspond to only the second lowest energy cluster as predicted by the FB potential demonstrating (as also observed in Figures 1 and 2) the close match with respect to ground-state energy prediction.

Structures of the Low-Energy Clusters. Prior to discussing the structures of the DFT-energy-minimized lowest energy $(SiO_2)_N$ ($N = 6-12$) clusters resulting from our procedure, it is useful to establish a consistent descriptive terminology. Throughout the full size range of clusters we find common motifs, which, although often regarded as defects for bulk silica, become, in the confining dimensions of a small cluster, inevitable structural mechanisms via which the cluster may lower its total energy. Three distinct motifs are prevalent which we define as: (i) a Si_2O_2 closed two-ring, (ii) a ═Si═O double-bonded oxygen termination, and (iii) local pairs of under-coordinated (≡Si−O) and over-coordinated (≡O) oxygen centers (for which the latter has three silicon atoms within $\sim$1.85 Å). Although (i) and (ii) are previously well documented for silica clusters, the combined state (iii) has not, to our knowledge, been described in the context of stoichiometric clusters before. It should be emphasized that clusters containing the structural motif (iii) do not seem to require any special electronic description, and, as with all clusters reported, are treated as closed-shell systems. This is in contrast, for example, to the isolated nonbonded oxygen (NBO) defect in bulk silica (≡Si−O•), which is known to be an open-shell photoluminescence center.[27] Furthermore, the structures and relative energies of clusters containing all three types of structural motifs are quite accurately predicted by our interatomic potential, pointing to a predominantly structural/atomistic, as opposed to electronic, stabilization of each center. A fuller structural, energetic, and electronic characterization of all motifs with respect to their occurrence in nanoscale silica structures is currently being undertaken and will be reported elsewhere.

Si_6O_{12}. Although it is generally accepted from manual conformer searches that the ground state for Si_6O_{12} is a linear D_{2h} chain of two-rings terminated at either end by a type (ii) ═Si═O center,[14] being also the form of the ground-state clusters for $(SiO_2)_N$ ($N \leq 5$),[12−14,18] this has never been tested by a search using a dedicated global optimization algorithm. As a first test of our BH/DFT methodology, we thus searched for low energy $(SiO_2)_6$ cluster conformations. Confirming previous work, we also found the $(SiO_2)_6$ two-ring chain, 4a, to be the lowest energy cluster; see Figure 4. In addition, the next highest cluster found, 4b, was 0.624 eV higher in energy than the chain having C_s symmetry and displaying centers of type (i), (ii) and (iii).

Si_7O_{14}. For $(SiO_2)_7$ we have previously applied our interatomic potential with a genetic algorithm global optimization scheme to establish two hitherto unknown clusters lower in energy than any previously reported.[19] Presently, using the BH global optimization procedure with our interatomic potential, we find the same low-energy clusters, and none lower in DFT-minimized energy, confirming this previous result; see Figure 4. Cluster 4c has C_s symmetry, with one type-(i) center and three type-(ii) centers but no type-(iii) centers, whereas cluster 4d has a 3-fold C_{3v} symmetry axis, with three type-(ii) centers and one type-(iii) center. It is noted that cluster 4d can be derived from cluster 4b by opening the 2-ring into a ═Si═O-terminated three-ring.

Si_8O_{16}. The lowest-energy $(SiO_2)_8$ cluster found by our methodology is a D_{2d} symmetric cross-like structure containing four type (ii) terminations and no other "defect" centers; see Figure 4, cluster 4e. Although we obtained this structure from a global optimization search, the same cluster has been proposed in the context of designing clusters via Si_3O_3-ring assembly.[16] Although the authors of this study[16] noted that cluster 4e was low in energy with respect to two other $(SiO_2)_8$ polymorphs, it was not claimed that the cluster was a ground-state cluster as in the present study, for which many other $(SiO_2)_8$ cluster polymorphs were also evaluated.

The simple form of cluster 4e seems to be strongly energetically favored with respect to other $(SiO_2)_8$ clusters, with the next lowest-energy $(SiO_2)_8$ cluster found being 1.422 eV higher in energy. Cluster 4e is also particularly low in energy with respect to clusters of similar size, where it is seen to have an anomalously-high binding energy (see Figures 1 and 2). On thermodynamic grounds, the cross-like Si_8O_{16} cluster thus can be thought of as a so-called "magic" cluster, which we predict should be able to be produced in cluster beams favoring low energy silica clusters.[18] It is worth noting that this cluster may

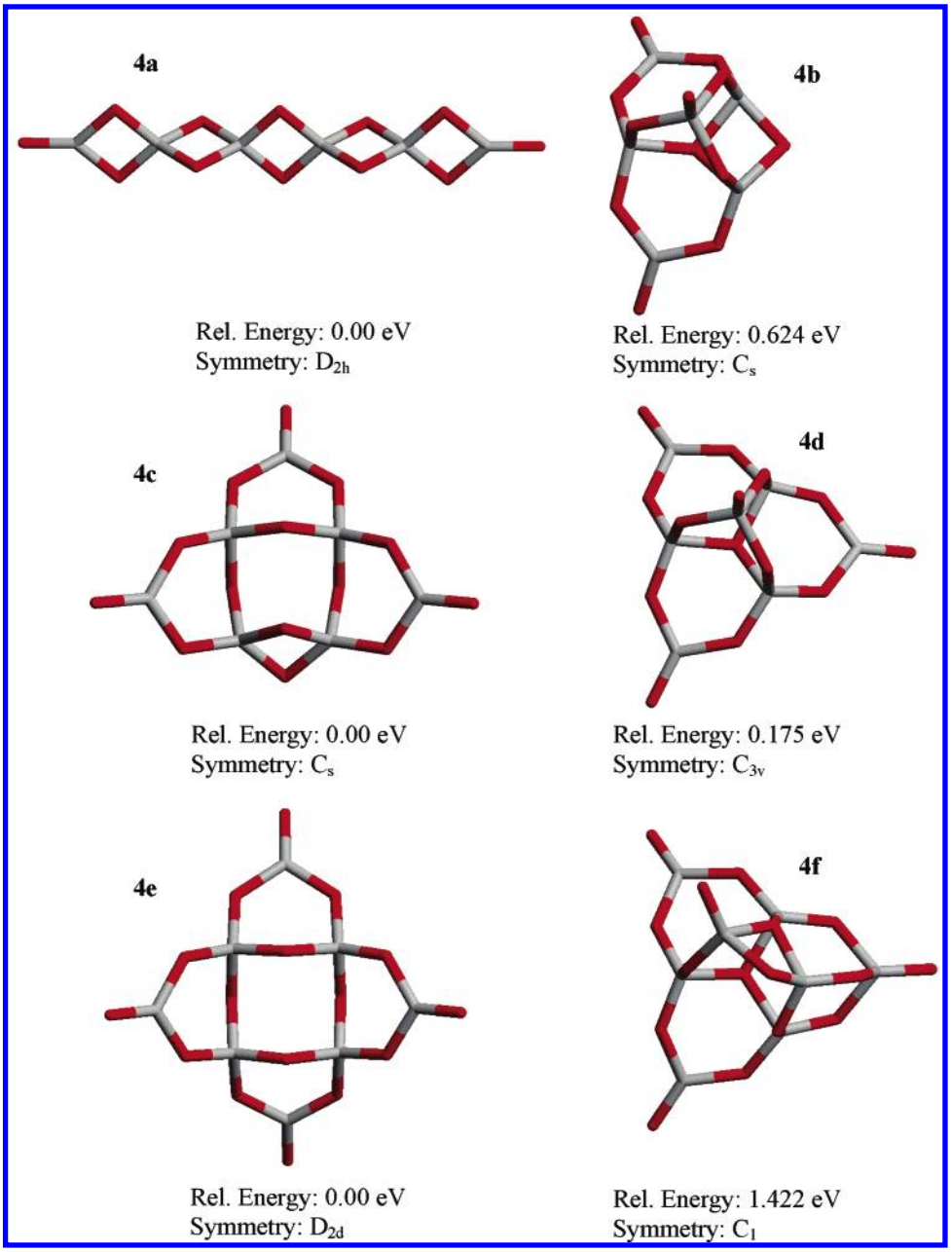

Figure 4. Structures of the lowest energy $(SiO_2)_6$ (4a, 4b), $(SiO_2)_7$ (4c, 4d), and $(SiO_2)_8$ (4e, 4f) clusters. The energies given are DFT-calculated energies relative to the lowest-energy cluster of that size. As for all cluster figures, lighter solid bars correspond to silicon atom positions and darker bars to oxygenation positions.

also be related to the high occurrence of "magic" $[(SiO_2)_8O_2H_3]^-$ clusters observed in laser ablation experiments.[28] The symmetric structure of the cluster 4e can be derived from that of cluster 4c by opening of the two-ring. In contrast cluster 4f is the least symmetric (C_1) of all the low energy clusters found and can be derived from cluster 4d by the addition of a two-ring, also inducing a second type (iii) center.

Si_9O_{18}. Progressing to $(SiO_2)_9$ clusters, the two lowest energy structures found (see Figure 5) take advantage of the low energy symmetric core of cluster 4e. The lowest-energy cluster 5a adds one SiO_2 unit to one of the terminating ═Si═O centers of cluster 4e forming a pendant two-ring and lowering the symmetry to C_s. The next lowest energy cluster 5b results from adding a SiO_2 unit onto the center of the cross form, creating two type (iii) centers and a structure having C_{2v} symmetry. Both structures are essentially degenerate, being exceedingly close in energy. The third lowest energy $(SiO_2)_9$ structure deviates from being an alteration to the 4e cluster, and is found to have a near-planar triangular C_{3v} symmetric form, consisting of alternating two-rings and ═Si═O-terminated three-rings.

$Si_{10}O_{20}$. For the lowest energy $(SiO_2)_{10}$ clusters found (see Figure 6) there appears to be a tendency to move away from cluster structures built upon smaller low-energy forms, with the two lowest energy structures, 6a and 6b, being distinct complex three-dimensional structures predominately formed from interconnected three-membered (Si_3O_3) silica rings. Both clusters display four ═Si═O centers, and have C_2 and C_s symmetries respectively. The third and fourth energetically lowest lying clusters, 6c and 6d, though also containing numerous three-membered rings, follow the patterns of SiO_2 addition to the $(SiO_2)_8$ cross-like cluster found for the two lowest-energy $(SiO_2)_9$ clusters (5a and 5b). For cluster 6c this results in simply the $(SiO_2)_8$ cross cluster with two pendant two-rings and C_{2v} symmetry, whereas for cluster 6d a novel highly symmetric (T_d)

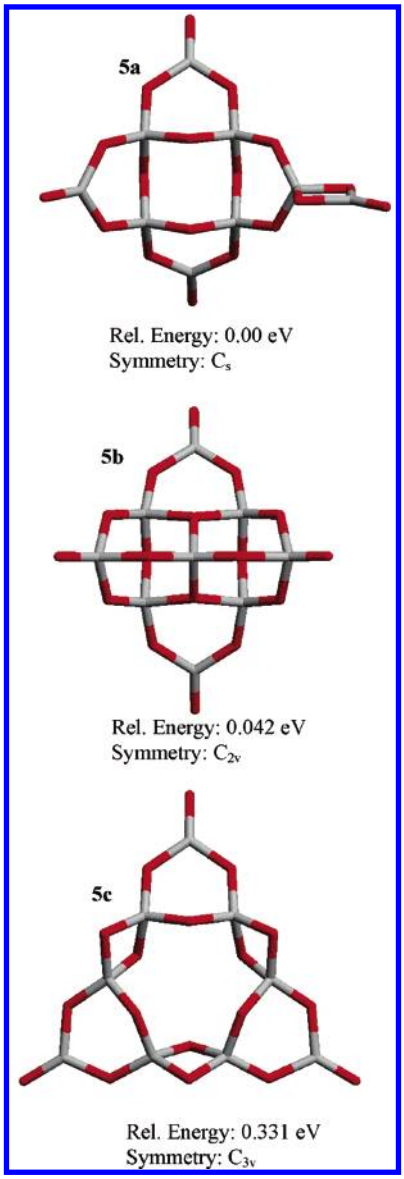

Figure 5. Structures of the lowest energy $(SiO_2)_9$ (5a, 5b, 5c) clusters. The energies given are DFT-calculated energies relative to the lowest energy $(SiO_2)_9$ cluster of that size.

cluster is formed displaying a "nano-diamond" structure with four type (iii) centers. As with clusters 5a and 5b, clusters 6c and 6d are nearly degenerate in energy. It should be noted that, although one can continue adding a two-rings to cluster 6c (although resulting in clusters that are not particularly low energy), one cannot simply continue the SiO_2 addition pattern 4e → 5b → 6d to form larger and larger SiO_2 nano-diamonds due to the eventual necessity of creating unstable four-coordinated oxygen atoms. It is of interest that although the emergence of the silica nano-diamond (6d) is the first low energy indication of a bulk crystalline motif, it is inherently only stable at the nanoscale. The diamond-like cluster structure is distinct from that known for the bulk SiO_2 phase of cristobalite in that in cluster 6d each individual oxygen and silicon atom map onto an atomic vertex of the diamond structure, whereas in the latter, the extended diamond structure is obtained by replacing the atomic vertices with SiO_4 tetrahedra.

$Si_{11}O_{22}$. The two lowest energy $(SiO_2)_{11}$ clusters, 7a and 7b, have a similar three-dimensional triangular structural form, and like clusters 6a and 6b have a significant number of three-membered silica rings but no distinct two-rings. Both clusters also have three similar terminations: one of type (ii), and two of type (iii), and have C_s and C_2 symmetries, respectively. The clusters are also very similar in total energy, differing by only 0.047 eV, being essentially degenerate. Neither cluster shows any definite indications of being built upon a smaller low-energy cluster, but are closest in form to low-energy clusters 4c and 5c also having an odd number of SiO_2 units.

$Si_{12}O_{24}$. The two lowest energy clusters found containing twelve SiO_2 units, 7c and 7d, have C_{2h} and C_2 symmetries, respectively, with both having a three-dimensional cylindrical form and formed predominately from four-membered silica rings. Each cluster has a type (iii) termination at each end joined together at a single four-ring. The two $(SiO_2)_{12}$ clusters represent two different ways of orientating the two four-ring-joined ends. Cluster 7c has its cylinder ends rotated 180 degrees with respect to each other, about the long axis of the cylinder, thus causing the two terminations to be diagonally opposed. On the other hand, cluster 7d has its ends rotated by 90 degrees with respect to each other causing a closer alignment of the two terminations and a corresponding increase in energy of 0.121 eV. As with the $(SiO_2)_{11}$ clusters, no SiO_2-addition scheme, based on previous low energy cluster forms, seems to simply describe the structure of the $(SiO_2)_{12}$ clusters though both have a significant number of constituent silica four-rings.

Discussion and Conclusions

All $(SiO_2)_N$ clusters reported for each particular N are distinguished from other clusters in that class by their particularly low energy. This thermodynamic stability, as deliberately chosen for via our methodology, corresponds to low-lying points on the respective potential energy surface (PES) of atomic configurations for each N. In itself, although pointing to the most energetically desirable cluster structures, this does not tell us how stable such clusters are to (i) thermal distortion to other cluster forms, and (ii) ionization and/or charge acceptance, (iii) reaction/coalescence with other clusters. Such concerns are particularly relevant for the production of clusters in high-energy beams, which aim to deliberately select discrete low energy clusters, often in an ionized state, and for using clusters as building blocks for novel materials. Although beyond the scope of the current study to assess all of these criteria in detail, for the new low energy clusters found we can simply extract the energetic positions of the highest occupied molecular orbital (ϵ_{HOMO}) and the lowest unoccupied molecular orbital (ϵ_{LUMO}) for each cluster from our DFT calculations, enabling us to give estimates of ionization energies (IP $= -\epsilon_{HOMO}$), electron affinities (EA $= -\epsilon_{LUMO}$), and relative reactivity via the HOMO−LUMO gap (ϵ_{LUMO}-ϵ_{HOMO}). In Figure 8 we show the IP, EA, and HOMO−LUMO gap of each of the lowest energy $(SiO_2)_N$ ($N = 1-12$) clusters, with respect to increasing N. For $N \leq 10$ all three parameters vary within a range of ~1.0 eV. For the chainlike isomers, $(SiO_2)_N$ ($N = 1-6$), the values are all fairly constant, whereas for $7 \leq N \leq 10$ a small odd-N/even-N alternation in the magnitudes of each parameter together with a small narrowing of the HOMO−LUMO gap is observed, corresponding with an increase in EA and decrease in IP values. For $N = 11$, however a large drop (>2.0 eV) in the HOMO−LUMO gap is observed, followed by a further smaller drop when going to $N = 12$. Relatively small HOMO−LUMO gaps are observed for most of the $(SiO_2)_N$, ($N = 11, 12$) clusters calculated, which tends to indicate a relatively higher susceptibility to charge transfer and thus bond formation between such clusters. In addition to the magnitude of the HOMO−LUMO gap, the nature of the electrostatic potential around a cluster

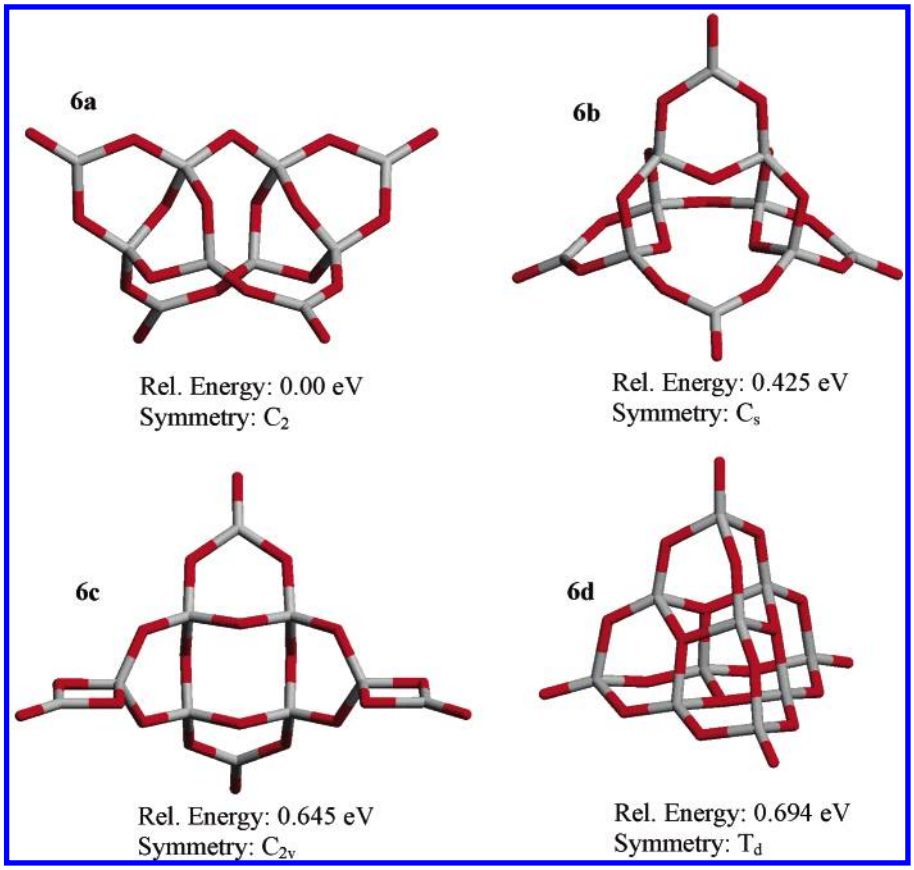

Figure 6. Structures of the lowest energy $(SiO_2)_{10}$ (6a, 6b, 6c, 6d) clusters. The energies given are DFT-calculated energies relative to the lowest energy $(SiO_2)_{10}$ cluster.

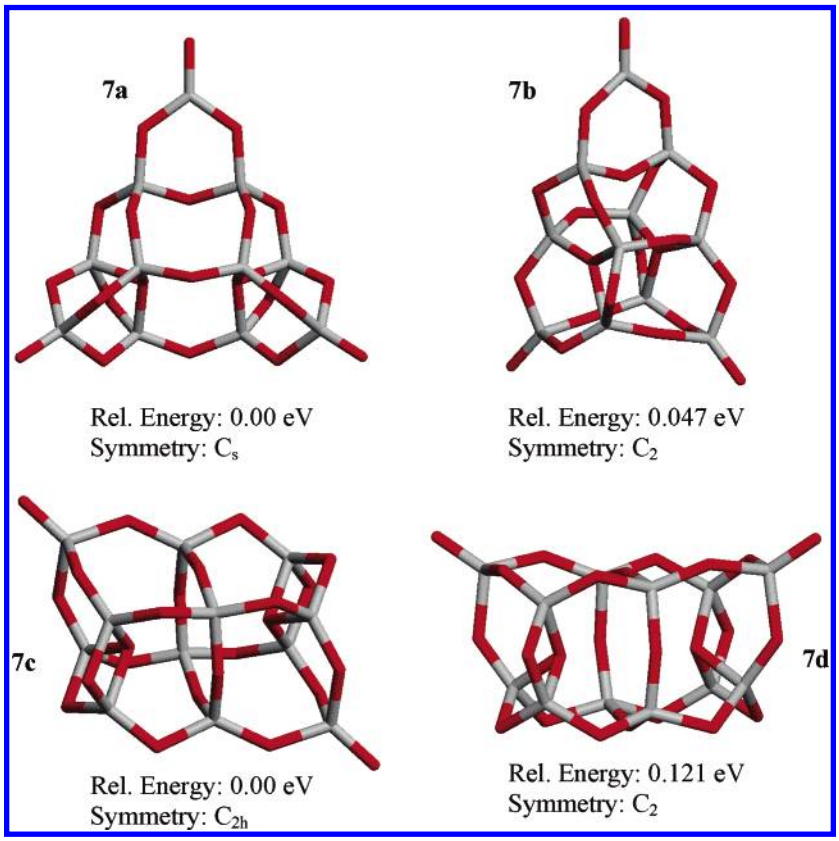

Figure 7. Structures of the lowest energy $(SiO_2)_{11}$ (7a, 7b) and $(SiO_2)_{12}$ (7c,7d) clusters. The energies given are DFT-calculated energies relative to the lowest energy cluster of that size.

also helps to determine its reactivity. For all calculated clusters, of all sizes, we have found that the vast majority possess terminating oxygen atoms of a type (ii) and/or type (iii) character. As Si−O and Si═O centers are inherently polar

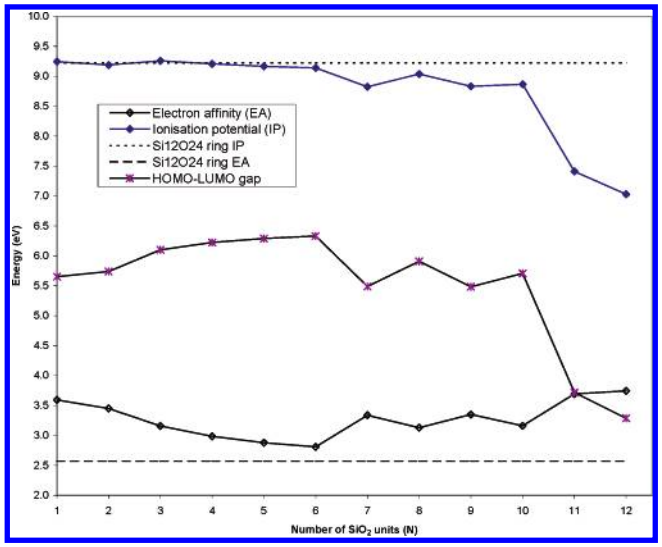

Figure 8. Comparison of the changes in ionization potential (IP), electron affinity (EA), and HOMO−LUMO gap of the lowest energy, $(SiO_2)_N$ ($N = 2-12$), clusters. For comparison the IP and EA of a ring-like fully coordinated cluster are also shown, see the dashed lines.

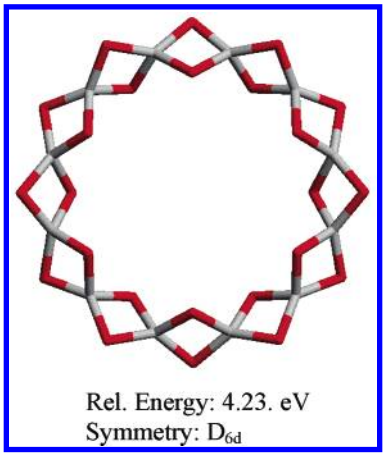

Figure 9. A fully coordinated $(SiO_2)_{12}$ ring-like cluster. The energy given is the DFT-calculated energy relative to the lowest energy $(SiO_2)_{12}$ cluster.

terminations this further promotes the tendency for clusters to align themselves and coalesce. In most cases, in fact, the frontier HOMO and LUMO orbitals are located around these accessible terminating centers, thus facilitating orbital overlap and therefore inter-cluster reactions to occur. The ease with which terminated clusters are likely to coalesce is further confirmed by calculations showing that the reaction between two Si═O centers is barrierless.[29]

In previous works we have explicitly demonstrated that silica clusters can be stabilized in a fully coordinated manner, that is, without terminating centers.[30] Such fully coordinated clusters inherently have no reactive Si−O or Si═O terminations and thus they also, correspondingly, often give rise to less pronounced differences in electrostatic potential that is, less polar. In a similar way fully coordinated clusters tend to favor more delocalized frontier orbitals, which can lead to a greater stabilization of the HOMO and an enhanced HOMO−LUMO gap. Both these effects are beneficial for lowering the intercluster reactivity and thus the resistance to coalescence. An example of a fully coordinated $(SiO_2)_{12}$ ring-like cluster also having a particularly high HOMO−LUMO gap (see the dashed boundary lines in Figure 8) is shown in Figure 9, which we have previously proposed as a candidate building block for new silica molecular materials. This cluster does not have a particularly low energy compared to energies of the lowest-lying $(SiO_2)_{12}$ clusters in Figure 3 (the ring cluster corresponds to $n = 29$), but its synthesis may be facilitated by using experimentally known precursors (e.g., ground-state two-ring chain clusters from molecular beams,[18] the two-ring chain bulk material silica−w[31]).

In summary, using a combined BH and DFT methodology, employing our dedicated nanoscale silica interatomic potential, we have explored the low-energy landscape of silica nanoclusters and proposed strong candidates for new ground-state clusters for $(SiO_2)_N$ ($N = 7-12$). In general the clusters bear little resemblance to known bulk silica polymorphs, although a nanodiamond analogue was discovered for $Si_{10}O_{20}$ (see cluster 6d). Some of the cluster structures can be thought of in terms of building upon smaller cluster structures (e.g., 4c → 4e), but, generally, the lowest energy clusters $(SiO_2)_N$ ($N = 7-12$), do not seem to follow any consistent growth pattern. This is quite unlike the $(SiO_2)_N$ ($N = 2-6$) ground state clusters which are simply formed from incremental additions of SiO_2 units to form increasingly longer two-ring chains. All investigated low-energy clusters are found to have reactive terminating groups, thus probably being unstable to coalescence when brought together. The larger clusters $(SiO_2)_N$ ($N = 11, 12$), in particular, were also found to have relatively small HOMO−LUMO gaps thus tending to increase their susceptibility to intercluster reactions. Although with increasing SiO_2 cluster size we would expect the gap to widen and eventually reach the limit of the wide band gap found for bulk silica, fluctuations about this mean behavior are well-known for the nanoscale (e.g., the IPs of small increasingly-sized metal nanoclusters[32]). We further show, however, that changes in the structure of silica nanoclusters can greatly affect the IP and the HOMO−LUMO gap, helping to tailor such clusters for use as building blocks for new materials. We present our lowest-energy silica clusters as benchmark ground-state clusters in the hope that this may stimulate challenges to our claim, and encourage further studies to further explore the properties of nanoscale silica.

Acknowledgment. We thank A. W. C. van den Berg, M. A. Zwijnenburg, and J. Wojdel for useful discussions.

References and Notes

(1) Ji, Q.; Iwaura, R.; Kogiso, M.; Jung, J. H.; Yoshida, K.; Shimizu, T. *Chem. Mater.* **2004**, *16*, 250.
(2) Zygmunt, J.; Krumeich, F.; Nesper, R. *Adv. Mater.* **2003**, *15*, 1538.
(3) Cornelissen, J. J. L. M.; Conner, E. F.; Kim, H.-C.; Lee, V. Y.; Magibitang, T.; Rice, P. M.; Volksen, W.; Sundberg, L. K.; Miller, R. D. *J. Chem. Soc., Chem. Commun.* **2003**, 1010.
(4) Sun, Q.; Kooyman, P. J.; Grossmann, J. G.; Bomans, P. H. H.; Frederik, P. M.; Magusin, P. C. M. M.; Beelen, T. P. M.; van Santen, R. A.; Sommerdijk, N. A. J. M. *Adv. Mater.* **2003**, *15*, 1097.
(5) Kim, Y. D.; Wei, T.; Wendt, S.; Goodman, D. W. *Langmuir* **2003**, *19*, 7929.
(6) Storm, A. J.; Chen, J. H.; Ling, X. S.; Zandbergen, H. W.; Dekker, C. *Nature* **2003**, *2*, 537.
(7) Davis, M. E. *Nature* **2002**, *417*, 813.
(8) Zhang, M.; Ciocan, E.; Bando, Y.; Wada, K.; Cheng, L. L.; Pirouz, P. *Appl. Phys. Lett.* **2002**, *80*, 491.
(9) Tong, L.; Gattass, R. R.; Ashcom, J. B.; He, S.; Lou, J.; Shen, M.; Maxwell, I.; Mazur, E. *Nature* **2003**, *426*, 816.
(10) Chen, J.-F.; Ding, H.-M.; Wang, J.-X.; Shao, L. *Biomaterials* **2004**, *25*, 723.
(11) Li, S.; Li, Z.; Yan, Y. *Adv. Mater.* **2003**, *15*, 1528.
(12) Lu, W. C.; Wang, C. Z.; Nguyen, V.; Schmidt, M. W.; Gordon, M. S.; Ho, K. M. *J. Phys. Chem. A* **2003**, *107*, 6936.
(13) Chu, T. S.; Zhang, R. Q.; Cheung, H. F. *J. Phys. Chem. B* **2001**, *105*, 1705.
(14) Nayak, S. K.; Rao, B. K.; Khanna, S. N.; Jena, P. *J. Chem. Phys.* **1998**, *109*, 1245.

(15) Harkless, J. A. W.; Stillinger, D. K.; Stillinger, F. H. *J. Phys. Chem.* **1996**, *100*, 1098.
(16) Lu, W. C.; Wang, C. Z.; Ho, K. M. *Chem. Phys. Lett.* **2003**, *378*, 225.
(17) Song, J.; Choi, M. *Phys. Rev. B: Solid State* **2002**, *65*, 241302(R).
(18) Wang, L.-S.; Desai, S. R.; Wu, H.; Nicholas, J. B. *Z. Physica D* **1997**, *40*, 36.
(19) Flikkema, E.; Bromley, S. T. *Chem. Phys. Lett.* **2003**, *378*, 622.
(20) Wales, D. J.; Doye, J. P. K. *J. Phys. Chem.* **1997**, *101*, 5111.
(21) Wales, D.J. *GMIN*: *A Program for Finding Global Minima*; www.wales.ch.cam.ac.uk/software.html
(22) Metropolis, N.; Rosenbluth, A. W.; Rosenbluth, M. N.; Teller, A. H.; Teller, E. *Chem. Phys*. **1953**, *21*, 1087.
(23) Wales, D. J.; Miller, M. A.; Walsh, T. *Nature* **1998**, *394*, 758.
(24) Doye, J. P. K.; Wales, D. J. *Phys. Rev. Lett.* **1998**, *80*, 1357.
(25) Becke, A. D. *J. Phys. Chem*. **1993**, *98*, 5648.
(26) Guest, M.F.; van Lenthe, J.H.; Kendrick, J.; Sherwood, P.; Amos, R.J.; Buenker, H.; van Dam, M.; Dupuis, N.; Handy, C.; Hillier, I.H.; Knowles, P.J.; Bonacic-Koutecky, V.; vaon Niessen, R.J.; Harrison, A.P.; Rendell, V.R.; Saunders, K.; Schoffel, A.; Stone, A.J.; Tozer, D. *GAMESS−UK*: *A Package of Ab Initio Programs.*
(27) Zyubin, A. S.; Glinka, Yu. D.; Mebel, A. M.; Lin, S. H.; Hwang, L. P.; Chen, Y. T. *J. Chem. Phys*. **2002**, *116*, 281.
(28) Xu, C.; Wang, W.; Zhang, W.; Zhuang, J.; Liu, L.; Kong, Q.; Zhao, L.; Long, Y.; Fan, K.; Qian, S.; Li, Y. *J. Phys. Chem. A* **2000**, 104, 9518.
(29) Kudo, T.; Nagase, S. *J. Am. Chem. Soc*. **1985**, *107*, 2589.
(30) Bromley, S. T.; Zwijnenburg, M. A.; Maschmeyer, Th. *Phys. Rev. Lett*. **2003**, *90*, 035502.
(31) Weiss, A. Z. *Anorg. Allg. Chem.* **1954**, *276*, 95.
(32) de Heer, W. A. *Rev. Mod. Phys.* **1993**, *65*, 611.